Reports

The Moon in Heiligenschein

Abstract. *An analysis of 25 photometric digital images of the moon has been carried out to obtain a single image in a new mapping parameter, the Heiligenschein exponent. The data necessarily represent a range of lunar phases, but all are within 10 hours of full moon. The new parameter characterizes the rate at which lunar features brighten as their local phase angles approach zero. Although considerable contrast is present in this parameter, there is only a small correlation with normal albedo. In particular, the large albedo difference between maria and highlands is not simply reflected in Heiligenschein differences, which are larger within each category of terrain than the difference between the Heiligenschein averages of each. A correlation with age may be present in both the maria and the highlands, but its determination will require separation into distinct geochemical provinces.*

Nearly all rough surfaces peak in reflected brightness in the back-scattering direction. In everyday experience, the result of this is the bright spot, or Heiligenschein, seen on the ground directly opposite the sun under such circumstances where it is not eclipsed by one's own shadow. The moon exhibits this effect strongly, and the spot was visually obvious from the orbiting Apollo command module. When seen from the earth, this effect is noticeable primarily as a variation over time in the brightness of the entire moon, with only a very subtle shading difference across the lunar face (*1*). Eclipse by the earth prevents astronomical observation of the phenomenon over its most pronounced range (*2*). The effect is thought to be closely associated with the degree of surface roughness (*3*) and is thereby a potential indicator of exposure age (*4*).

My object in the study reported here has been (i) to form a mappable parameter associated with the strength of the Heiligenschein phenomenon and (ii) to display it over the near face of the moon. In order to avoid ambiguities in the physical interpretation of actual numerical results, I have avoided an ad hoc approach to the problem of forming a mappable parameter (*5*). Instead, I have formed the parameter in terms of a mathematical model of the light-scattering process, even though the model is empirical rather than physical.

The investigation requires intercomparison of detailed lunar photometry acquired at different times. A total of 25 photoelectrically calibrated photographic plates ranging in mean phase angle (*1*) from 2° to 4.5° was used (*6*). Those aspects of the computer processing which involve the transformations between picture frame coordinates in the digitized images and selenographic coordinates, the computation of lighting and viewing parameters for a particular selenographic coordinate at a specific time, and general photometric reduction are the same as for the recent digital albedo file I have produced and are detailed therein (*7*). The extension of computational techniques peculiar to the present study involves the central modeling equations

$$I = (F_\odot/\pi)\rho[\Phi(g, i, \epsilon)]^C \quad (1)$$

$$\Phi(g, i, \epsilon) = [\Phi_0(g)]\left[\sum_{n=0}^{9} a_n\left(\frac{\cos\epsilon}{\cos i}\right)^n\right] \quad (2)$$

where I is the surface brightness (*8*), $F_\odot$ is the radiant solar flux at the earth's orbit (*9*), ρ is the normal albedo (*10*), g is the local phase angle (*1*), i is the angle of incidence (*11*), ϵ is the angle of emergence (*12*), and $\Phi_0(g)$ is the so-called standard photometric function near zero phase angle (*13*). The set of coefficients a_n is determined by a least-squares calculation and is assumed not to be selenographically variable (*14*). The quantity C is the Heiligenschein exponent (*15*), which I have identified as the mappable Heiligenschein parameter and the only term in Eqs. 1 and 2 in addition to ρ which is selenographically variable (*16*). There are two sets of coefficients a_n, discriminated on the basis of whether (cos ϵ/cos i) is greater or less than unity (Table 1).

Table 1. Coefficients of the polynomial power used in the lunar photometric function.

n	a_n	
	(cos ϵ/cos i) > 1	(cos ϵ/cos i) < 1
0	26.8123	171.2085
1	−62.3666	−711.6860
2	12.3383	881.3830
3	52.1569	−25.1183
4	−6.3474	−328.0940
5	−31.1410	−661.5440
6	−3.1637	1100.8200
7	17.8499	−395.3400
8	−4.8527	−84.4292
9	−0.2861	53.8100

On the assumption that Eqs. 1 and 2 can predict all the photometric observations for the right choice of a distribution of ρ and C over the lunar surface, that distribution has been formed. The choice of the form of the equations may seem somewhat unusual inasmuch as (cos ϵ/cos i) is never very far from unity for the present range of observations. I make no pretense of justifying the form on any basis other than the a posteriori argument that it works reasonably well; there remains relatively little broad, gradual, systematic variation in C across the final image in that parameter (*17*). The remnant of this artifact that does exist may be somewhat annoying, but it does not impede visual detection of terrain differences as expressed in Heiligenschein. All other modeling techniques that I tried led to partial images (*18*). A more elaborate model-fitting procedure in which the Hapke improved photometric function was used might provide more satisfactory results (*19*), but the point-by-point application of the more elaborate analytical form and the associated nonlinear least-squares analysis would increase computation time prohibitively.

Inasmuch as the variation in C depends on small differences in brightness, the random photometric error produces a noisier image in C than it does in ρ. Those errors that arise from residual inaccuracies in the interframe transformation matrices are also largely random. I have examined them and have found them to be less than a pixel except within about 4 percent in the radius of the limb, where the Heiligenschein image should not be taken seriously. The distribution on the sky of the zero-phase point relative to the center of the moon does not have radial symmetry (*20*). A systematic error resulting from a coupling of albedo gradient to misregistration through this selection effect can result in adjacent positive and negative anomalies. As I will show below, this is probably responsible for the abrupt boundary in the Heiligenschein mapping of Aristarchus,

0036-8075/78/0616-1265$00.50/0

although the crater is too large for its distinction to be completely explained away in this manner.

The results of this analysis, in both ρ and C, are shown in Fig. 1. Some striking features indicated by the Heiligenschein image in comparison with an ordinary image in normal albedo are apparent, but there is not a consistent difference between the uplands and the maria. Within the maria themselves, Mare Imbrium and Mare Nectaris are relatively mottled in appearance, whereas Mare Tranquillitatis and the major portions of Mare Crisium and Mare Humorum appear most homogeneous. Some mare border materials are very subdued in the Heiligenschein surge; that is, they appear quite dark in Heiligenschein image, most notably on the south side of Mare Frigoris and Sinus Roris and the west sides of Mare Crisium and Oceanus Procellarum. Craters Manilius and Plinius are quite subdued, as is Posidonius, which is morphologically older, and parts of the Copernicus rim material. Within the uplands, the Alpes, the Caucasus, and the Pyreneaus are abundant in features of subdued Heiligenschein surge. Tycho does not stand out sharply, nor, somewhat surprisingly, does the Tycho ray system. The Tycho rim material shows a weaker effect than either the crater interior or the ray system. The most intense Heiligenschein surges occur around Aristarchus and at an extremely bright spot, "Hell," 150 km northeast of Tycho, near Walter.

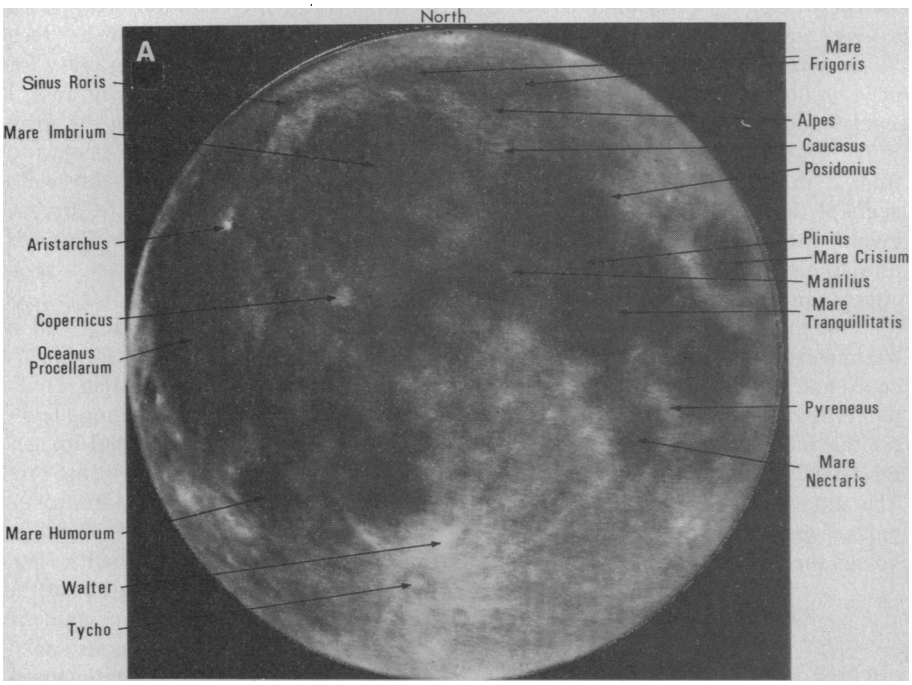

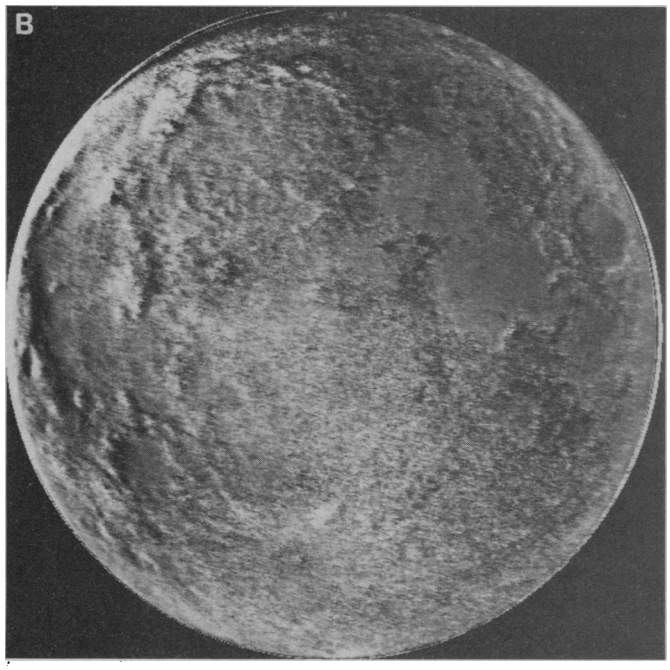

Fig. 1. (A) An image of the moon in normal albedo, in which the correction for the geometry of observation/illumination is peculiar to each selenographic coordinate rather than a lunar average. (B) An image of the moon in Heiligenschein exponent, which is monotonic in the relative upsurge in brightness as true local full moon ($g = 0$) is approached. For visual calibration, the value of C is about 2.1 at Hell, near Walter, and 0.2 at the extensive minimum between Manilius and Plinius. The lunar average value of C, excluding the limb regions, is 0.95.

A definitive interpretation of these data will require a long-term effort in which they are compared with other results. For example, it is tempting to conclude that the present observations form an independent basis for the indication that the mare border materials are relatively young, as are the rims of the small sharp craters, deduced from relatively weak Heiligenschein. Posidonius, then, although older, might be thought to show similarly weak Heiligenschein because it may be chemically different, since it is not as distinctly placed in the maria. Tycho, presumably younger than Posidonius because of its relative sharpness of appearance, would then be indicative of a third geochemical or petrological category, since it is a case of more nearly average strength of the Heiligenschein effect and is well into the highlands. This scheme begins to present almost as many categories as there are observations when we attempt to incorporate Aristarchus and the region near Walter. The solution to this problem will be enhanced by incorporation of these data into the Lunar Consortium data bank in Flagstaff.

Terrestrial mapping of the Heiligenschein phenomenon is of potential value. Although the instrumentation best adapted to accomplish it would be vastly different from what I have used, a relatively undemanding degree of sophistication can be envisioned. An area-scanning photometer is one possibility. Because of the small field about the antisolar direction occupied by significant Heiligenschein, a large number of passes would be required for complete reconnaissance; thus a long-term program with the use of a small satellite would be necessary, rather than an airborne operation. Completeness of coverage would be effected by the incommensurability between orbital period and relative rotational period of the earth. The most obvious application relates to the mapping of vegetation, which exhibits a Heiligenschein phenomenon obvious to anyone who flies. There is no reason to believe that such mapping should be of no geological significance, however, particularly over the more arid regions of the earth. In this case also, association with other kinds of data would be of paramount importance.

ROBERT L. WILDEY
Department of Astronomy and Physics, Northern Arizona University, Flagstaff 86001, and *Branch of Astrogeologic Studies, U.S. Geological Survey, Flagstaff*

References and Notes

1. In the change of perspective from lunar orbit to the earth's surface as observing station, the angular size of the moon in the field of view is greatly reduced. But a nearly negligible change in the very much greater distance to the sun occurs, so that the mapping of phase angle onto the sky as circles concentric about the antisolar direction is unaffected in scale. (The local phase angle of an observed landmark is the angle between the observer and the sun as it would be measured from that landmark.)
2. The Heiligenschein region of the lunar photometric function was first detected from the earth in 1964 by T. Gehrels, T. Coffeen, and D. Owings [*Astron. J.* **69**, 826 (1964)], wherein it was referred to as the "opposition effect," and also, but at a lower signal-to-noise ratio, by R. Wildey and H. Pohn (*ibid.*, p. 619); see also J. Van Diggelen, *Planet. Space Sci.* **13**, 271 (1965). Direct observation of the entire eclipsed region based on the use of Apollo orbital photography was carried out by H. Pohn, H. Radin, and R. Wildey [*Astrophys. J.* **157**, L193 (1969)]. Although the angular spread of the earth is greater than that of the sun as seen from the moon, the angular spread of the Apollo command module is negligible compared to that of the sun and is a negligible source of obscuration and diffraction when seen from the moon in transit on the solar disk. R. Wildey and H. Pohn [*Astrophys. J.* **158**, L129 (1969)] by similar methods confirmed that the magnitude of the effect was variable over the lunar surface. Laboratory studies of the optical properties of Apollo-returned samples by B. O'Leary and F. Briggs [*J. Geophys. Res.* **75**, 6532 (1970); *ibid.* **78**, 792 (1973)] confirmed and extended these studies.
3. The relevant scale of roughness a priori includes all radii of surface curvature in the range from just below resolution (a few hundred meters at astronomical resolution or a few meters at Apollo resolution) to just above the wavelength of light, or about 1 μm. In practical terms, the effective range of the size distribution of soil particles (tens to hundreds of micrometers) is strongly dominant. The existence of the Heiligenschein phenomenon is then implied by the disappearance of visible shadows at a phase angle of zero. For explicitly quantitative theories of the effect, see B. Hapke [*J. Geophys. Res.* **68**, 4571 (1963); *Astron. J.* **71**, 333 (1966)] and W. Irvine [*J. Geophys. Res.* **71**, 2931 (1966)]. The applicability of these theories is somewhat marginal.
4. The exposure age of primary consequence is the cumulative bombardment by meteorites and micrometeorites. The pitting effect of the smaller meteoroids governs roughness in an obvious way, but all bombardment by consolidated rock affects roughness through the deposition of dust particles (with vacuum welding) and larger debris. To the extent that hard radiation may damage crystal structure and, through darkening, may reduce further the significance of higher order scattering of light, the importance of shadowing is enhanced. In both considerations there is a rationale for the Heiligenschein to increase in strength with time.
5. For example, if one merely mapped the slope of the relation between brightness increase and phase angle for small phase angles (this was done), the result would show a very strong systematic trend correlated with the variation over the lunar surface of the orientation of the local surface normal with respect to the sunward and earthward average directions. The trend would swamp the variations associated with geologic variety. But it could be removed afterward by d-c plus high-pass spatial filtering of the image.
6. The plates used were Eastman Kodak II a-E and 103a-E through a Wratten-4 filter; I took the photographs at the Newtonian focus of the 61-cm reflector of the Northern Arizona University Astrophysical Observatory.
7. R. L. Wildey, *Moon* **16**, 231 (1977). The method of achieving absolute calibration by normalizing to the total lunar flux is especially important to the need in the present investigation for accurate photometric differences over time.
8. The quantity I is also a specific intensity and has the units of heterochromatic power per unit area in a plane perpendicular to the direction of I, per unit solid angle surrounding that direction.
9. Power per unit area, appropriately spectrally weighted.
10. Normal albedo is the ratio of the observed surface brightness under the condition that $g = i = \epsilon = 0$ to the surface brightness of an ideal surface (Lambertian) which absorbs no energy and presents a directionally invariant specific intensity.
11. The angle of incidence is the angle between the local surface normal and the sunward direction. I have assumed the equivalence of the surface normal and the local vertical.
12. The angle of emergence is the angle between the surface normal and the direction to the observer [see also (*11*)].
13. This function is derived from Apollo Heiligenschein photometry as a nominal photometric function for use near zero phase angle only, in which the dependence on i and ϵ has been neglected. It has been published in tabular form by R. Wildey [*Observatory* **96**, 235 (1976)]. It varies from a value of 1 at $g = 0°$ to 0.83 at $g = 4°$.
14. The ten coefficients, a_n, were determined by the method of least squares in which the set of reduced observations consisting of I for a given selenographic coordinate was used to form the set of all possible ratios of observed I for that coordinate. In this way the quantity ρ disappears when Eqs. 1 and 2 are used to represent the new observational set. The two sets of all such observations on (i) the bright-limb side of the center-of-face and (ii) the terminator side were then formed to provide two separate regions of function definition, within which separate sets of coefficients a_n, obtained from two separate least-square fits, were found. The quantity C was set equal to unity throughout the entire procedure.
15. The quantity C was determined by a separate least-square calculation for each selenographic coordinate corresponding to a pixel of the final digital output map. With the a_n already determined, Eqs. 1 and 2 were used directly with the 25 observed values of I to determine ρ and C for each selenographic coordinate.
16. In stating that ρ and C are the only terms that are selenographically variable, I exclude, of course, the selenographically correlated variations in g, i, and ϵ that are due to changes in illumination; these variations are fully determined and are not of geologic origin.
17. Nevertheless, the form of Eqs. 1 and 2 was not chosen arbitrarily. I originally expected that little, if any, dependence of Φ on i and ϵ would have to be considered, but, when $\Phi = \Phi_0$ was tried, the results were unsatisfactory. It was already know that $\partial\Phi/\partial i$ and $\partial\Phi/\partial\epsilon$ were negligible near $g = 0$, although $\partial\Phi/\partial g$ is about 0.03 to 0.06 per degree. This follows from the fact that the observed Heiligenschein spot retains circular symmetry as it approaches the lunar horizon in Apollo orbital photography [see also (*18*)]. The determination of C involves such small brightness differences that $\partial^2\Phi/\partial i\partial g$ and $\partial^2\Phi/\partial\epsilon\partial g$ are nonnegligible. Even these terms had been found small under conditions away from low sun angle and low observing angle [R. Wildey, *NASA Spec. Publ. 315* (1973)]. The functional form chosen lends itself readily to these properties of the derivatives. It also retains the definitional property whereby $\Phi = 1$ for $g = i = \epsilon = 0$. The reduction to a dependence on (cos ϵ/cos i) is equivalent to a dependence on the single angle called luminance longitude, in keeping with the long-known lunar behavior over the general range of lighting and viewing parameters [see M. Minnaert, in *Planets and Satellites*, G. Kuiper and B. Middlehurst, Eds. (Univ. of Chicago Press, Chicago, 1961), p. 221]. Unfortunately, I found no simple way of achieving these properties while guaranteeing obedience to the reciprocity principle. That was left to its inherent expression in the data and the numerics of a best fit. (The reciprocity principle, which deals with covariance under the interchange of observer and illuminator, is a corollary of the second law of thermodynamics and is discussed by Minnaert.)
18. A different effect is the systematic increase in the contrast in C, exemplified by western Oceanus Procellarum as one nears the limb, which was observationally biased in favor of being the bright limb. The result combines with residual shading variations to give the image an appearance of being "lit from the west." I tentatively interpret this to mean that the intrinsic differences in Heiligenschein between different types of terrain genuinely maximizes for low sun and lower observer. This would imply that the Apollo-based observation of the retention of circular symmetry by the Heiligenschein spot on approaching the lunar horizon cannot be generalized with completely adequate precision.
19. See Hapke in (*3*). The present observations support Hapke's prediction of sunward limb-brightening, which earlier observers have not detected.
20. Without considerable mobility with regard to the observatory at which the data is gathered, such uniformity for observations extending to small phase angle cannot be achieved except over long periods of time.

21. I thank Dr. H. Kieffer, whose very helpful criticism resulted in the complete rewriting of this report. This research was supported by NASA contract W13,130.

12 September 1977; revised 13 January 1978

Oxygen Isotope Composition of Subglacially Precipitated Calcite: Possible Paleoclimatic Implications

Abstract. *Isotopic analyses of subglacially precipitated calcite from near a modern temperate glacier show that the* $\delta^{18}O$ (= $^{18}O/^{16}O$ *relative to standard mean ocean water) of the calcite records the* $\delta^{18}O$ *of the ice from that glacier. It may therefore be possible to determine the* $\delta^{18}O$ *of Pleistocene ice sheets on the basis of isotopic analyses of calcite formed under that ancient ice. This, in turn, would allow estimation of the* $\delta^{18}O$ *of Pleistocene oceans and correction of the paleotemperature scale based on foraminiferal oxygen isotopic analyses.*

Thin calcite-rich coatings are widespread on calcareous bedrock exposed by actively retreating temperate glaciers (*1*). They have been reported near modern glaciers in central Norway (*2*), the Alps (*2, 3*), the Rocky Mountains (*4, 5*), and the Himalayas (*5*), as well as on bedrock formerly glaciated by the Pleistocene Fennoscandian ice sheet (*6*). These deposits form by precipitation of $CaCO_3$ from subglacial waters as a direct consequence of the glacier sliding process (*5*).

We suggest here that the oxygen isotope composition of calcite that formed under a glacier records the oxygen isotope composition of the ice from that glacier and is relatively independent of the calcite composition of the bedrock. Analyses of calcite precipitated under Pleistocene ice sheets may therefore lead to an estimate of the oxygen isotope composition of the ice sheet. Such an achievement would be of special interest because it could greatly improve the interpretation of apparent foraminiferal paleotemperatures by allowing estimation of the $\delta^{18}O$ of Pleistocene oceans.

Temperate glaciers slide over their irregular beds by the combined actions of plastic deformation and of pressure melting and refreezing. In the latter process,

0036-8075/78/0616-1267$00.50/0